Indonesian Journal of Material Research
e-ISSN: 2987-1654
Vol. 1, No. 3, November 2023

Indonesian Journal of MATERIAL RESEARCH

Research Paper

Ca/Al and Mg/Al LDH Supported on Biochars As Effective Adsorbent and Highly Regeneration Ability for Phenol Removal from Aqueous Solution

Erni Salasia Fitri[1], Try Nanda Yunita[1], Risfidian Mohadi[2], Aldes Lesbani[1,2]*

[1] *Research Center of Inorganic Materials and Complexes, Sriwijaya University, Palembang, 30139, Indonesia*
[2] *Master of Materials Science, Graduate Program, Sriwijaya University, Palembang, 30139, Indonesia*
***Corresponding author**: aldeslesbani@pps.unsri.ac.id

Abstract
This research conducted a composite of Ca/Al and Mg/Al Layered double hydroxide with Biochar material using co-precipitation method. Characterization results were carried out with various analyses including XRD, FT-IR, and BET. The results of XRD analysis on Ca/Al-BC showed peaks at 10-11° and 22°, while the Mg/Al-BC material showed peaks at 11.41° (003), 22.95° (002), 34.05° (012) and 60.2° (116). The FT-IR analysis showed that Ca/Al and Mg/Al LDH materials composited with Biochar have functional groups of −OH, nitrate ions, C=O, C−H, C−O, and M−O. BET analysis results show an increase in surface area in Ca/Al and Mg/Al LDH materials after composite with biochar from 29.333 m^2/g to 158.291 m^2/g in Mg/Al-BC, while in Mg/Al-BC there is an increase from 23.150 m^2/g to 111.404 m^2/g. The Ca/Al-BC and Mg/Al-BC composite materials have better stability than Ca/Al and Mg/Al LDH materials that can be used up to the fifth cycle. Hydrogen bonding and π-π interaction between the adsorbent and the aromatic ring on phenol can affect the adsorption process.

Keywords
LDH, Biochar, Composites, Phenol Adsorption, Regeneration

Received: 25 September 2023, Accepted: 27 November 2023
https://doi.org/10.26554/ijmr.20231316

1. INTRODUCTION

Phenol is one of the organic compounds found in industrial wastewater that can harm all organisms, animals, plants, and humans if accumulated on the food chain. Phenols can be found in many industrial wastes, including petrochemicals, coal processing, pharmaceuticals, polymer resins, and pesticide industries (Bazrafshan et al., 2016; Xie et al., 2020). At a low concentration of 5 $\mu g.L^{-1}$, phenol compounds can be damaging to plants, aquatic organisms, and even humans. If phenol compounds are contaminated in the human body in the long term at concentrations between 10 and 240 $mg.L^{-1}$ can cause mouth irritation, visual impairment, and indigestion (Dehmani et al., 2022; Dehbi et al., 2020). In addition, exposure to phenols in humans results in a variety of diseases, including skin burns, liver and kidney damage, nervous system paralysis, and cancer (Abdel-Gawwad et al., 2023). Therefore, many researchers have tackled various ways to remove phenol compounds.

Various types of methods can be applied such as physical, chemical, and biological methods in handling the removal of organic and inorganic pollutants. Several methods that have been used to remove phenol include chemical oxidation, photodegradation, ion exchange, electrocoagulation, coagulation-flocculation, membrane filtration, adsorption, advanced oxidation processes, and others (Buhani et al., 2018; Igwegbe et al., 2019; Chowdhury et al., 2021; Lee et al., 2019). However, the most widely used method is adsorption. The adsorption method has several advantages over other methods including its simple operation process, the availability of abundant adsorbent precursors, relatively low cost, level of efficiency, and high effectiveness of environmentally friendly as well as the absence of side effects of toxic substances (Sahu et al., 2021; Dehmani et al., 2021; Wang et al., 2016; Li et al., 2022). A recent study conducted by Abdel-Gawwad et al. (2023) on phenol adsorption using red clay brick, Haydari et al. (2023) using reduced graphene oxide, Lammini et al. (2022) using cobalt oxide, Wei et al. (2023) used activated carbons produced from antibiotic mycelial residues and traditional biomass, and Yuliasari et al. (2023) MgCr layered double hydroxide/ microcrystalline cellulose composite.

Layered double hydroxide (LDH) is a layered material that has a positively charged layer between which there are anions and water known as interlamellar (Das et al., 2023). These materials have advantages such as low raw material cost, high adsorption capacity, and easy synthesis. However, LDHs are not suitable for use in regeneration processes, they can peel off during the process. Therefore, it is necessary to modify LDH with a stable structure material such as biochar (Missau et al., 2021), so that it has high adsorption capacity and regeneration

ability. Modification of layered double hydroxide composites using biochar has been carried out by Juleanti et al. (2021); Sun et al. (2022) which adsorbed Cr(VI) with adsorbents in the form of biochar-based Ca/Al and Mg/Al composites. Based on the results of his research, materials that have been modified, namely CaAl-Biochar and MgAl-Biochar materials can increase the value of adsorption capacity on LDH materials. Ca/Al LDH which was originally only 89.286 $mg.g^{-1}$ increased to 588.235 $mg.g^{-1}$, while Mg/Al increased from 86.957 $mg.g^{-1}$ to 426.316 $mg.g^{-1}$ after composite with biochar. In addition, the modification results can also increase the surface area of the material, where Ca/Al LDH from 47.027 m^2/s to 150.987 m^2/s and Mg/Al LDH from 23.150 m^2/s to 111.404 m^2/s.

This study conducted the synthesis of Ca/Al and Mg/Al layered double hydroxide supported on biochar (BC) composites as adsorbents on phenol adsorption. The synthesis material was characterized using X-Ray Diffraction (XRD) analysis, Fourier Transform Infrared Spectroscopy (FT-IR), and Brunauer Emmet Teller (BET) analysis. The material is applied as an adsorbent for the phenol adsorption process by observing several free variables such as the influence of pH, the influence of time, the influence of concentration and temperature, and its regeneration.

2. EXPERIMENTAL SECTION

2.1 Chemicals and Instrumentation

The materials used in this study such as Aluminum Nitrate Nonahidrat ($Al(NO_3)_3.9H_2O$), water, Hydrochloric Acid (HCl), biochar obtained from rice husks, buffer pH 10, phenol (C_6H_5OH), kallium Hexacyanoferrate(III) ($K_3[Fe(CN)_6]$), magnesium nitrate hexahydrate ($Mg(NO_3)_2.6H_2O$), sodium hydroxide (NaOH), calcium nitrate tetrahydrate ($Ca(NO_3)_2.4H_2O$), sodium chloride (NaCl), dan 4-aminoantipyrine ($C_{11}H_{13}N_3O$). Then it was characterized using an X-Ray Rigaku Miniflex-600 diffractometer, BET Surface Area Analyzer Micrometric ASAP Quantachrome, Shimadzu Prestige-21 FTIR Spectrophotometer, and Biobase Spectrophotometer UV-Visible BKUV1800PC.

2.2 Synthesis of Ca/Al LDH and Mg/Al LDH

Solution of $Ca(NO_3)_2.4H_2O$ 100 mL 0.75 M mixed with 100 mL $Al(NO_3)_3.9H_2O$ 0.25 M for Ca/Al LDH synthesis. A sodium hydroxide 2 M (NaOH) solution was added slowly to pH 10 and heated at 65°C. For 24 hours at a temperature of 65°C, constant stirring is carried out. The precipitate is obtained then filtered and washed with a neutral pH using water. For 24 hours at 100°C the residue was dried using the oven. Mg/Al LDH synthesis was performed with a 100 mL solution of $Mg(NO_3)_2.6H_2O$ mixed with 100 mL $Al(NO_3)_3.9H_2O$, slowly added a mixture of 2 M pH 10 NaOH solution and stirred for 24 hours. Then the mixture is heated for 24 hours at a temperature of 80°C. The precipitate is then filtered and washed using water to a neutral pH and dried using an oven for 24 hours at 100°C. It is then characterized using XRD, FT-IR, and BET analysis.

2.3 Preparation of Ca/Al-BC and Mg/Al-BC Composites

The coprecipitation method was used in the preparation of the composites by keeping the pH at a constant level. A 30 mL of $Ca(NO_3)_2.4H_2O$ or $Mg(NO_3)_2.6H_2O$ solution with a concentration of 0.75 M was mixed with 30 mL of $Al(NO_3)_3.9H_2O$ solution with a concentration of 0.25 M, then mixed with 2 M NaOH solution and adjusted the pH to reach a value of 10. The mixture was stirred for 1 hour, then 3 g of biochar was added and heated for 72 hours at 80°C. Through the use of an oven, the precipitate formed was filtered and dried for 24 hours at 100°C. The next process involved characterization using XRD, FT-IR, and BET analysis.

2.4 Study of pH point zero charge (pHpzc)

The pHpzc study was carried out by adding 20 mL of NaCl solution having a concentration of 0.1 M to each 0.02 g adsorbent, with pH settings varying from 2, 3, 4, 5, 6, 7, 8, 9, 10, to 11. NaOH and HCl solutions, both with a concentration of 0.1 M, were added to the NaCl solution to adjust its pH. After mixing, the mixture was stirred for 24 hours, then filtered, and the pH of the filtrate was measured. Next, each component was analyzed by creating a graph that visualizes the relationship between the initial pH and the final pH to determine the pH pzc value.

2.5 Adsorption Process

Adsorption was explored through various treatments, including manipulation of pH, adsorption contact duration, concentration, and initial solution temperature. Modification of pH (2-11) had a significant impact on the adsorption process to determine the optimal pH point. A total of 20 mL of phenol was introduced into an Erlenmeyer with 0.02 g of adsorbent at a concentration of 10 mg/L, and mixing was carried out for two hours. The control of adsorption contact time was key to determine the window of optimal conditions when the influence of pH was kept constant. Temperature (30, 40, 50, 60, and 70°C) and concentration (10, 15, 20, 25, and 30 mg/L) were used to investigate the effect of adsorption in terms of initial concentration and temperature. In this experiment, 20 mL of phenol was mixed with 0.02 g of adsorbent in an Erlenmeyer, then stirred for a period of time that was considered ideal. The filtrate was measured using a UV-Vis spectrophotometer, with the initial step being the complexation of the phenol filtrate, followed by absorbance measurements. A beaker containing 1 mL of phenol was filled with 0.1 mL of 2% 4-amino antipyrine reagent solution, 0.1 mL of 8% potassium hexacyanoferate(III) solution, and 3 mL of buffer solution with pH 10, then homogenized and left for 15 minutes.

2.6 Desorption Process and Regeneration

Accompanying the desorption process is the regeneration process. Ultrasonics are used to desorb the adsorbent from the solution. The regeneration procedure is then completed by adding 0.1 g of adsorbent to a phenol solution containing 10 mg/L, stirring for 2 hours, and measuring the filtrate's absorbance with a UV-Vis spectrophotometer before drying it in the oven. Following the use of dry adsorbents in the desorption process, the

© 2023 The Authors.

regeneration procedure is repeated five times.

3. RESULTS AND DISCUSSION

Ca/Al LDH is obtained from the synthesis of calcium nitrate tetrahydrate compounds with aluminum nitrate nano hydrate and Mg/Al LDH is obtained from the synthesis of magnesium nitrate hexahydrate compounds with aluminum nitrate nano hydrate where each synthesized layered double hydroxide material is regulated to reach pH 10 with the addition of sodium hydroxide. The LDH was obtained and then each of them was characterized using X-Ray Diffraction (XRD) analysis (Ahmad et al., 2022). The results of the analysis display the diffractogram as shown in Figure 1. According to Helard et al. (2018) diffraction characteristics in Ca/Al LDH are around 11°(003) and 23° (006). The results of research conducted by Juleanti et al. (2021) obtained peaks of Ca/Al LDH diffraction at 10.18° (003) and 20.61° (006). Figure 1(a) shows the Ca/Al LDH diffractogram in this study with diffraction angles at 10.06° (003) and 20.06° (006). This shows that the results of the Ca/Al LDH synthesis have been successfully carried out.

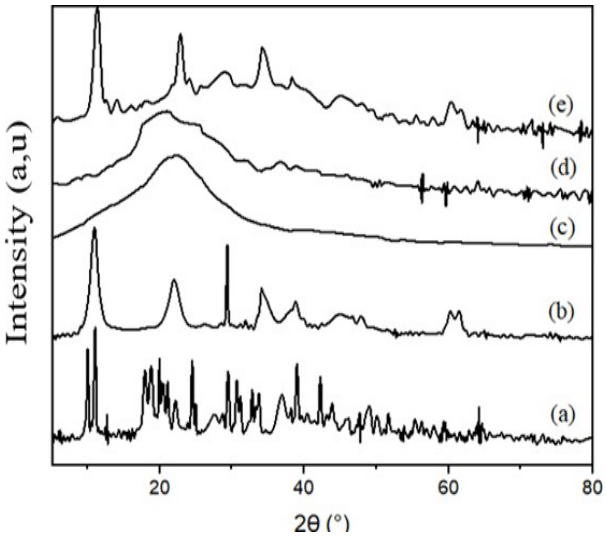

Figure 1. Diffraction patterns of Ca/Al LDH(a), Mg/Al LDH(b), Biochar(c), Ca/Al-Biochar(d), and Mg/Al-Biochar(e)

Figure 1(b) displays a Mg/Al LDH diffractogram with diffraction angles at 10.98° (003), 29.39° (002), 34.31° (012), 60.04° (110), and 61.51° (116). XRD results for Mg/Al LDH showed the presence of diffraction peaks at 11.47° (003), 22.86° (002), 34.69° (012), 60.33° (110), and 61.62° (116) consisting of divalent and trivalent ions. Based on the results of this study, the synthesis of Mg/Al LDH has been successfully carried out. LDH is modified using BC to form Ca/Al-BC and Mg/Al-BC composites which aims to make the adsorbent reusable in the adsorption process. The biochar used comes from rice husks. The pattern of the BC diffractogram is shown in Figure 1(c) which produces the characteristic BC at an angle of 22.30° (002). According to the research of Badri et al. (2021) in biochar there is a widening peak of about 21-26° (002).

The results of the XRD analysis of the Ca/Al-BC composite are shown in Figure 1(d) where the peak is not so visible around 10-11° and at the peak of 22° this is because the synthesis results obtained are not good. The results of the XRD analysis of the Mg/Al-BC composite are shown in Figure 1(e) where there are peaks at 11.41° (003), 22.95° (002), 34.05° (012) and 60.2° (116). The study conducted by Badri et al. (2021) obtained the results of the Mg/Al-BC composite diffractogram where there were peaks at 11.47° (003), 22.86° (002), 34.69° (012) and 61.62° (116). This suggests that the synthesis of MgAl/BC composites has been successfully carried out.

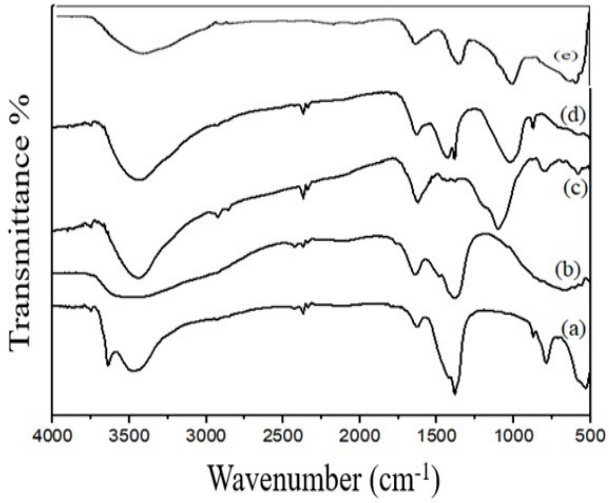

Figure 2. FT-IR Spectrum of Ca/Al-LDH (a), Mg/Al-LDH (b), Biochar (c), Ca/Al-Biochar (d), and Mg/Al-Biochar (e)

FT-IR (Fourier Transform-Infra Red) analysis is carried out to determine the functional groups contained in the material. Figure 2(a) shows the Ca/Al LDH spectrum containing vibration at wave number 3479.58 cm^{-1} indicating the presence of the -OH group. The wave number at 1381.03 cm^{-1} indicates the presence of nitrate ions, in addition to the vibration in the wave numbers 786-424 cm^{-1} which indicates the interaction between metal and oxygen (M−O) namely Ca−O and Al−O and in wave number 1620.21 which indicates the vibration of the −OH group from water. The results of research conducted by Mohadi et al. (2021), FT-IR spectrum for Ca/Al LDH there are nitrate ions at 1381 cm^{-1}. The presence of stretching vibration and bending vibration of the OH group derived from water contained in wave numbers 3480 cm^{-1} and 1620 cm^{-1}. The vibrations of M^{2+} and M^{3+} are below 800 cm^{-1} (Bouteraa et al., 2020). This proves that the synthesis of Ca/Al LDH was successfully carried out in this study. The spectrum contained in Figure 2(b) shows the results of FT-IR analysis for Mg/Al LDH which has a peak at wave number 3471.87 cm^{-1} indicating the bending vibration of the −OH group of water, wave number 1381.03 cm^{-1} which indicates the presence of nitrate ions. The vibration is found at 1635.64 cm^{-1} which indicates the presence of an −OH cluster of water. The interaction between metal and oxygen (M−O) namely

© 2023 The Authors.

Mg−O and Al−O is at a wave number below 1000 cm^{-1}. The results of the FT-IR BC analysis are shown in Figure 2(c) where there is a vibration at wave number 3448.72 cm^{-1} which indicates the presence of vibration from −OH, at wave number 1620.21 cm^{-1} shows the vibration of C=O, the vibration in the wave number 2368.59 cm^{-1} comes from the C−H bond. The research of Badri et al. (2021) has a vibrational peak at a wavelength of 2376 cm^{-1} derived from the C−H bond of the biochar. There are vibrations of ult and bending at 3448 cm^{-1} and 1635 cm^{-1} indicating the presence of −OH bonds coming from water.

Figure 2(d) shows the FT-IR spectrum for the Ca/Al-BC composite where there is vibration in the wavenumber region of 3400 cm^{-1} indicating the presence of the −OH group. The vibration of the wave number 800-400 cm^{-1} indicates an interaction between metal and oxygen. The increase in the peak intensity of vibration in wave numbers is due to an increase in the number of biochars used in composites. The presence of vibration in the Ca/Al-BC composite material at wave number 1381.03 cm^{-1} indicates vibration of nitrates. Figure 2(e) shows the FT-IR spectrum for the Mg/Al-BC composite where there is vibration from the −OH group at wave number 3471 cm^{-1}. The presence of nitrate ions in the wave number 1381 cm^{-1}. There is an interaction between metal and oxygen in areas below 1000 cm^{-1}. According to research that has been conducted by Badri et al. (2021) shows the presence of vibrations at the wave number 1381 cm^{-1} which indicates the presence of the N=O group of the nitrate anion, 3447 cm^{-1} indicates the presence of the –OH group derived from absorbed water, 1010 cm^{-1} there is a C−O group from the biochar, and 1635 cm^{-1} there is an O−H group derived from water.

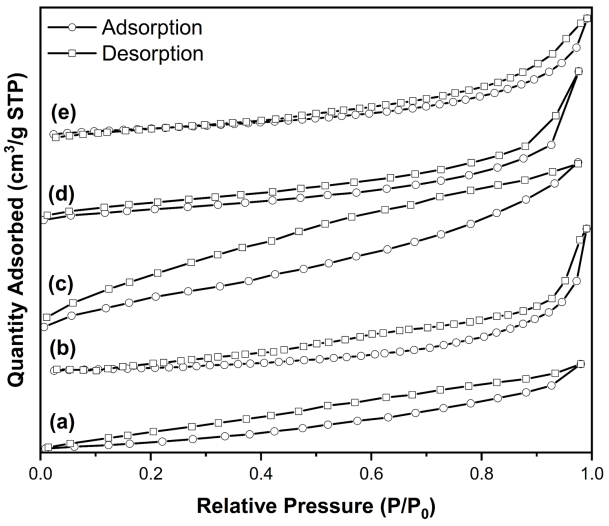

Figure 3. BET Profile of Ca/Al-LDH (a), Mg/Al-LDH (b), Biochar (c), Ca/Al-Biochar (d), and Mg/Al-Biochar (e)

BET analysis is performed to determine the specific surface area of a material and the pore distribution of the material using nitrogen desorption adsorption (Asnaoui et al., 2022). The nitrogen adsorption-desorption data on each adsorbent can be seen in Figure 3 and the bet measurement data can be seen in Table 1. Based on the profile in Figure 3, it shows the phenomenon of hysteresis which occurs due to differences in adsorption and desorption pathways. Figure 3 shows adsorption-desorption isotherms of type IV due to the presence of mesoporous-sized particles with strong hysteresis activity on the interaction of adsorbents with adsorbates (Shaji and Zachariah, 2017; Alsamman et al., 2017).

Table 1. Data of BET Analysis

Adsorbents	Surface Area (m^2/g)	Pore Volume (cm^3/g)	Pore Diameter (nm)
Ca/Al	29.333	0.007	13.033
Mg/Al	23.150	0.092	36.000
Biochar	50.936	0.025	12.089
Ca/Al-Biochar	158.291	0.017	12.474
Mg/Al-Biochar	111.404	0.062	10.918

Table 1 shows that Ca/Al LDH has a surface area of 29.333 m^2/g, a pore volume of 0.0072 cm^3/g, and a pore diameter of 13.033 nm. Based on research that has been conducted by Wei et al. (2020) the surface area of Ca/Al LDH is 7.6 m^2/g, the pore volume is 0.07 cm^3/g and the pore diameter is 57.6 nm. This proves that the results of the Ca/Al LDH synthesis in this study have a larger surface area but a smaller pore volume and diameter than previous studies. According to research conducted by Zhou et al. (2021), Mg/Al LDH has a surface area of 51.91 m^2/g, a pore volume of 0.2039 cm^3/g, and a pore diameter of 15.709 nm while the synthesis results in this study resulted in a surface area of Mg/Al LDH of 23,150 m^2/g, a pore volume of 0.092 cm^3/g and a pore diameter of 36,000 nm. This shows that the surface area and pore volume of the synthesis results in this study have a smaller size but have a larger pore diameter compared to previous studies.

Ca/Al and Mg/Al LDH undergo an increase in surface area after being formed into a modified composite using biochar because biochar has a large surface area that can reduce layered double hydroxide agglomeration. A decrease in pore volume and pore diameter in composites can occur due to the intercalation of biochar in a layered layered double hydroxide that will cause the pores to become smaller and more regular (Badri et al., 2021).

The study's materials underwent a pHpzc test, with the outcomes displayed in Figure 4(a). The pH pzc values for the materials Ca/Al LDH, Mg/Al LDH, BC, Ca/Al-BC, and Mg/Al-BC are 4.7, 5.12, 7.28, 8.74, and 9.13, respectively, according to the findings of the pH pzc test on each material. Figure 4(b) shows the test results for each substance, which were used to estimate the ideal pH during the phenol adsorption procedure. Figure 4(b) shows that the ideal pH for Ca/Al LDH is 6 and for Mg/Al LDH is 5. pH 7 is the ideal level for BC, Ca/Al-BC, and Mg/Al-BC (Xie et al., 2020).

To ascertain the ideal time for the phenol adsorption process

© 2023 The Authors.

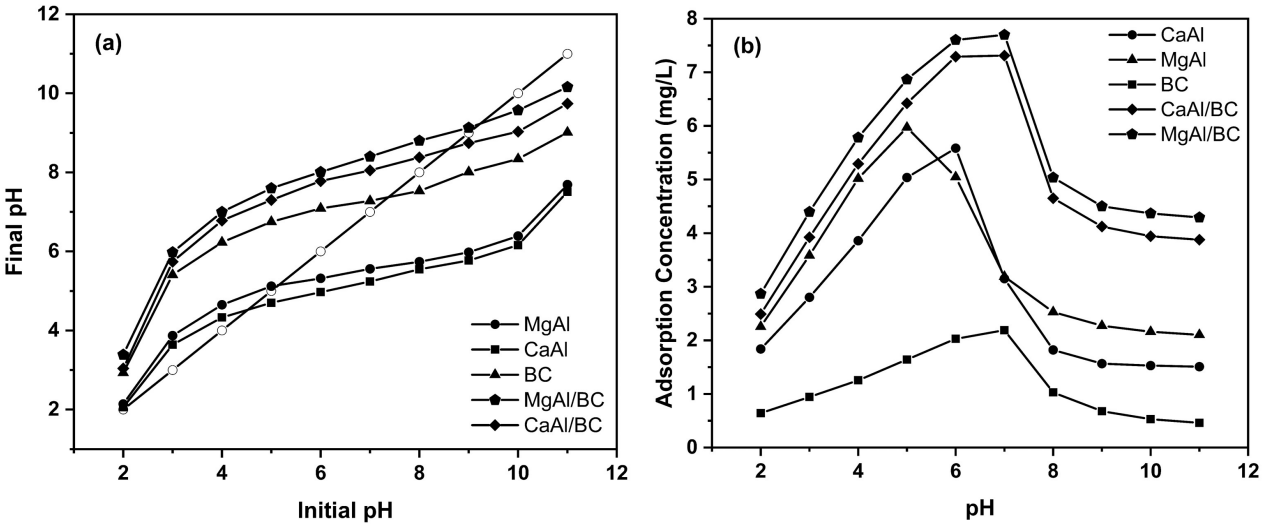

Figure 4. pHpzc of materials (a) and Effect of pH on Adsorption Process (b)

Table 2. Adsorption Kinetic Parameters

Adsorbents	Initial Concentration (mg/L)	Qe_{exp} (mg/L)	PFO			PSO		
			Qe_{calc} (mg/L)	R^2	k_1	Qe_{calc} (mg/L)	R^2	k_2
Ca/Al	15	8.443	2.919	0.866	0.037	8.562	0.999	0.039
Mg/Al		7.83	4.641	0.931	0.029	8.244	0.998	0.012
Biochar		8.981	2.4	0.868	0.035	9.091	0.999	0.045
Ca-Al/BC		8.613	1.752	0.845	0.031	8.666	0.999	0.072
Mg-Al/BC		8.925	2.090	0.794	0.036	8.985	0.999	0.064

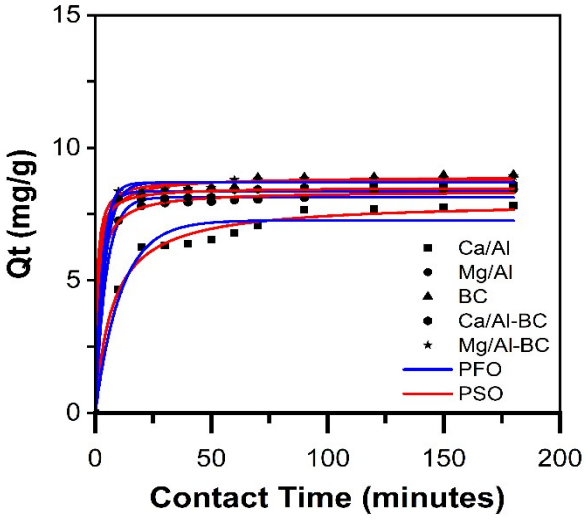

Figure 5. Adsorption Kinetic Models

on the adsorbent, the influence of time on phenol adsorption is investigated. The effect of adsorption time is investigated using a phenol solution with a concentration of 15 mg/L that has been adjusted in pH in accordance with the optimum pH of phenol, namely pH 6 for adsorbent Ca/Al LDH, pH 5 for adsorbent Mg/Al LDH, and pH 7 for adsorbent BC, layered double hydroxide composite Ca/Al-BC, and Mg/Al-BC Figure 5 depicts the impact of adsorption time on phenol.

Based on the data in Figure 5, the longer the adsorption time, the more the amount of phenol concentration that is adsorbed will also increase. At minute 60 is the optimum time for adsorbents Ca/Al-BC and Mg/Al-BC in the phenol adsorption process where in more than 60 minutes the adsorbed concentration tends to be constant. At the 70^{th} minute the biochar adsorbent reaches its optimum time where after more than the 70^{th} minute the concentration tends to be constant. The optimum time for Mg/Al LDH adsorbents is at minute 90 and Ca/Al LDH is at minute 120.

Table 2 contains kinetic model data for the pseudo-first order and pseudo-second order adsorption of phenol onto layered double hydroxides of Ca/Al LDH, Mg/Al LDH, BC, Ca/Al-BC, and Mg/Al-BC composites. The results of phenol adsorption time effect data are utilized to calculate the adsorption rate using the kinetic equation of pseudo first order and pseudo second order. The value of the coefficient of determination (R^2) approaching 1, the value of the kinetic rate (k), and the similarity between the Qe values of the experiment and the calculation can all be used

© 2023 The Authors.

Table 3. Adsorption Isotherm Parameters

Adsorbents	Adsorption Isotherm	Adsorption Constant	Temperature (°C) 30	40	50	60	70
Ca/Al LDH	Langmuir	Q_{max}	19.960	20.040	16.779	19.194	10.183
		kL	0.702	0.449	0.299	0.194	0.101
		R^2	0.855	0.875	0.906	0.955	0.952
	Freundlich	*n*	9.714	14.225	57.143	71.429	25.381
		kF	1.737	1.866	2.169	2.451	2.652
		R^2	0.938	0.961	0.939	0.955	0.885
Mg/Al LDH	Langmuir	Q_{max}	15.221	14.837	17.794	19.231	21.552
		kL	0.517	0.347	0.252	0.186	0.130
		R^2	0.971	0.976	0.977	0.978	0.981
	Freundlich	*n*	9.091	3.557	9.048	7.188	5.632
		kF	2.291	2.857	3.107	2.338	3.080
		R^2	0.994	0.987	0.984	0.999	0.999
Biochar	Langmuir	Q_{max}	28.490	23.041	21.097	24.752	24.154
		kL	1.139	0.583	0.315	0.206	0.127
		R^2	0.965	0.985	0.994	0.986	0.992
	Freundlich	*n*	4.574	9.017	18.656	18.115	32.467
		kF	1.737	1.866	2.169	2.451	2.651
		R^2	0.875	0.917	0.938	0.892	0.892
Ca/Al-BC	Langmuir	Q_{max}	37.037	32.258	55.555	52.632	58.749
		kL	1.8	1	0.280	0.121	0.058
		R^2	0.986	0.993	0.998	0.952	0.995
	Freundlich	*n*	3.141	4.370	5.854	8.389	13.568
		kF	1.737	1.866	2.169	2.451	2.651
		R^2	0.999	0.999	0.979	0.974	0.999
Mg/Al-BC	Langmuir	Q_{max}	30.303	28.089	31.847	27.621	27.798
		kL	1.5	18.714	7.913	8.112	9.542
		R^2	0.806	0.957	0.933	0.864	0.806
	Freundlich	*n*	3.281	0.186	0.119	0.091	0.072
		kF	1.737	1.866	2.169	2.451	2.651
		R^2	0.864	0.964	0.974	0.920	0.869

to identify the kinetic model in the adsorption process. Based on the results of the kinetic data used to calculate the adsorption rate in Table 2, it can be observed that each adsorbent's coefficient of determination (R^2) tends to be more suited when used with second-order pseudo-equations, as shown by a determination value (R^2) that is close to 1. Table 2 contains data on the kinetic rates (k) of the Ca/Al LDH, Mg/Al LDH, BC, Ca/Al-BC, and Mg/Al-BC composites. This table demonstrates that all adsorbents tend to have modest values for k_1 while having larger values for k_2. Phenol adsorption follows the pseudo second order equation when analyzed from the similarity between the Qe result of the experiment and the Qe calculation.

Data on the effect of adsorption concentration and temperature have been collected using various types of adsorbents, including Ca/Al LDH, Mg/Al LDH, BC, Ca/Al-BC, and Mg/Al-BC composites. The purpose of this data collection was to evaluate the adsorption isotherm parameters by applying the Langmuir and Freundlich equations. The Langmuir equation was used to determine the value of the Langmuir isotherm equilibrium constant (KL) and the maximum adsorption capacity of adsorbent (Qm) (Chen et al., 2021). On the other hand, the Freundlich equation provides the Freundlich isotherm equilibrium constant (KF) and adsorption degree of freedom (n). The use of the Langmuir equation is recommended when the adsorption process occurs in the form of a single layer or monolayer, and there are interactions in the adsorbate molecules (Liu et al., 2021; Onder et al., 2020). In contrast, the Freundlich equation is more suitable for adsorption processes that occur in several layers or multilayers, where there is no association and dissociation of adsorbate molecules (Kurniawati et al., 2015). Assessment of this parameter is done by considering the regression value (R^2). Complete data on phenol adsorption isotherms on various types of adsorbents can be found in Table 3.

From the data in Table 3, the phenol adsorption process against the layered double hydroxide adsorbent Ca/Al LDH and BC follows the Langmuir adsorption isotherm model as evi-

© 2023 The Authors.

Table 4. Comparison of Adsorption Capacity on the Phenol Removal by Several Adsorbents

Adsorbent	Adsorption Capacity (mg/g)	References
Cobalt Oxide	8.10	(Lammini et al., 2022)
Granular Activated Carbon from Coconut Shell	17.54	(Desmiarti et al., 2019)
Mangifera kemanga Blume Seed	3.86	(Mardiah et al., 2022)
Activated Carbon from Rice Husk Activated by $ZnCl_2$	3.937	(Anshar et al., 2016)
Luffa cylindrica Fibers	10.37	(Abdelwahab and Amin, 2013)
Nano-Zinc Oxide/Activated Carbon-$ZnCl_2$ Composite	17.45	(Allwar et al., 2021)
Coconut Shell Activated Carbon	19.02	(Ho and Adnan, 2021)
Natural Clays	10.00	(Dehmani et al., 2021)
Rice Husk Ash	13.98	(Mandal et al., 2019)
Fe_3O_4/Chitosan/ZIF-8 Nanocomposite	6.43	(Keshvardoostchokami et al., 2021)
Magnetic Double-Network Nanocomposite Hydrogel	16.52	(Nakhjiri et al., 2021)
Chitosan/Calcined Eggshell	10.82	(Tamang and Paul, 2022)
Lignite	6.22	(Liu et al., 2021)
Cationic Surfactant Modified Attapulgite (Gemini Modified ATP)	24.26	(Wang et al., 2022)
Gelatin Aerogel-Containing Al-Metal Organic Framework	16.56	(Kim et al., 2023)
Polyacrylonitrile Nanofiber Membranes	38.4	(Nthunya et al., 2019)
Ca/Al-BC	58.749	This work
Mg/Al-BC	31.847	This work

denced by the value of the linear regression coefficient in the Langmuir isotherm equation close to 1. Mg/Al, and Ca/Al-BC and Mg/Al-BC composites tend to the Freundlich adsorption isotherm model. Based on the maximum adsorption capacity (Qm) value in Table 3 data, it is known that Ca/Al-BC composite adsorbents have the largest adsorption capacity. The adsorption capacity of phenol on Ca/Al, Mg/Al, BC, Ca/Al-BC, and Mg/Al-BC were 20.040, 21.552, 28.49, 58.749, and 31.847 mg/g, respectively. The comparison of adsorption on the phenol removal by several adsorbents is shown in Table 4. The effectiveness of phenol removal can be seen by the value of adsorption capacity on Ca/Al-BC and Mg/Al-BC which is larger compared to other adsorbents. This proves that the material in this study can be used as an effective adsorbent for phenol removal.

The thermodynamic results of the adsorption of phenol using adsorbents Ca/Al LDH, Mg/Al LDH, BC, Ca/Al-BC, and Mg/Al-BC in Table 5 were endothermic. This can be seen from the enthalpy value which is positive which means it requires energy. In Ca/Al LDH and Mg/Al LDH the largest entropy at a concentration of 25 mg/L was 0.094 kJ/mol and 0.093 kJ/mol. The entropy value in BC and Mg/Al-BC with a concentration of 20 mg/L experienced the largest increase in enthalpy, namely 0.099 kJ/mol and 23.565 kJ/mol. In Ca/Al-BC, the entropy value of the concentration of 15 mg/L is the largest, which is 22.476 kJ/mol. This indicates that the greater the entropy value, the greater the degree of irregularity. Gibbs free energy is negatively valued indicating the adsorption process takes place spontaneously and with increasing temperature causes a decrease in Gibbs free energy (Sahmoune, 2019; Palapa et al., 2020).

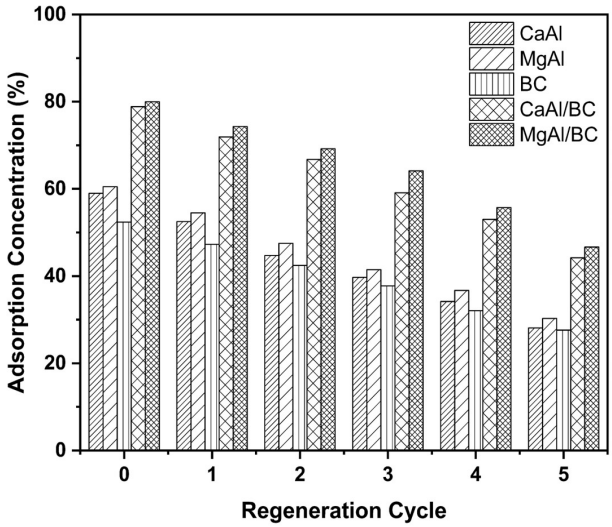

Figure 6. Regeneration Ability of Materials

The regeneration process can be carried out after performing the adsorption and desorption process using water with an ultrasonic device. Figure 6 shows the results of the regeneration of adsorbents Ca/Al LDH, Mg/Al LDH, BC, Ca/Al-BC, and Mg/Al-BC against phenols. The results from Figure 6 show that the adsorbed percent for layered double hydroxide composite adsorbents Ca/Al-BC and Mg/Al-BC is higher than that of adsorbents Ca/Al LDH, Mg/Al LDH, and BC. Ca/Al LDH and Mg/Al LDH decreased drastically in the third regeneration on phenol

© 2023 The Authors.

Table 5. Adsorption Thermodynamic Parameters

Adsorbents	Concentration (mg/L)	T (K)	Qe (mg/g)	ΔH (kJ/mol)	ΔS (J/mol. K)	ΔG (kJ/mol)
Ca/Al LDH	25	303	19.466	25.570	0.094	-2.955
		313	20.409			-3.896
		323	21.221			-4.837
		333	22.240			-5.779
		343	23.070			-6.720
Mg/Al LDH	25	303	20.202	24.587	0.093	-3.494
		313	21.164			-4.421
		323	22.013			-5.347
		333	22.579			-6.274
		343	23.334			-7.201
Biochar	20	303	14.070	27.977	0.099	-1.936
		313	15.013			-2.923
		323	16.051			-3.910
		333	17.051			-4.897
		343	18.013			-5.884
Ca/Al-BC	15	303	10.198	22.476	0.080	-1.776
		313	11.019			-2.576
		323	11.576			-3.376
		333	12.198			-4.177
		343	12.972			-4.977
Mg/Al-BC	20	303	15.645	23.565	0.088	-3.027
		313	16.391			-3.904
		323	16.976			-4.782
		333	17.777			-5.660
		343	18353			-6.537

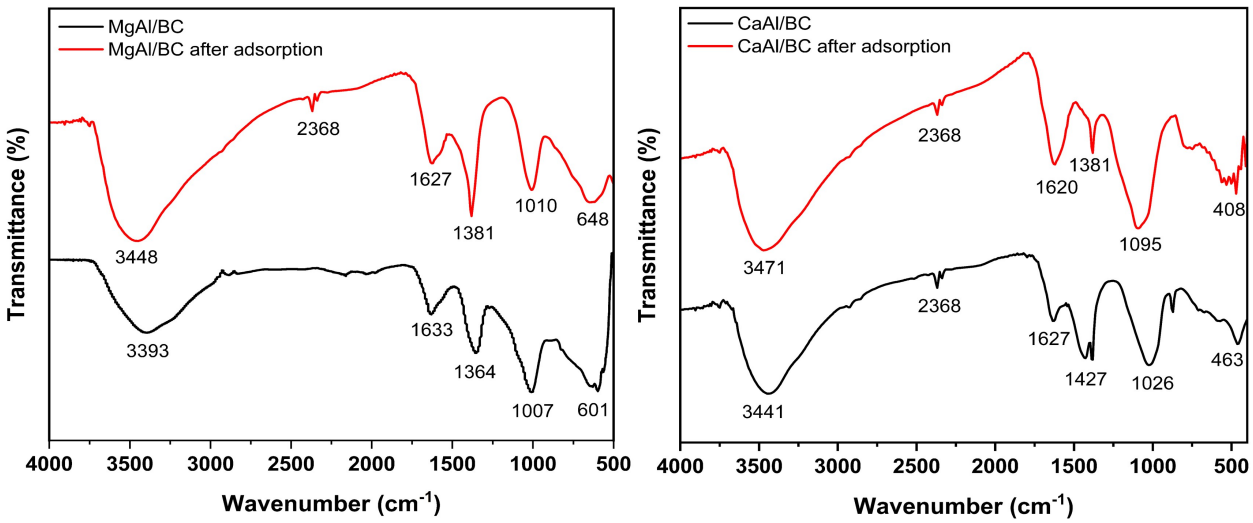

Figure 7. FTIR Spectrum of Ca/Al-BC and Mg/Al-BC After Phenol Adsorption

© 2023 The Authors.

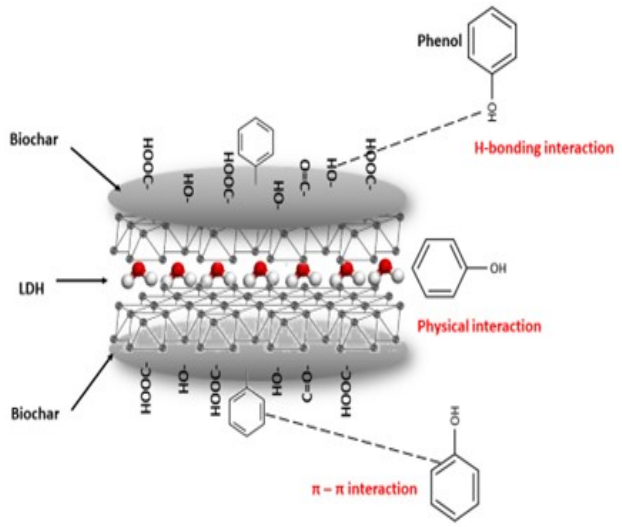

Figure 8. Adsorption Mechanism of Phenol on Ca/Al-BC and Mg/Al-BC

adsorption. This is because the Ca/Al LDH and Mg/Al LDH are exfoliated so that they are less stable and cannot carry out the phenol adsorption process in subsequent regeneration. Ca/Al-BC and Mg/Al-BC did not show a drastic decrease in adsorbed percent until the fifth cycle with percent efficiency of 44.2 and 46.67% respectively.

FTIR spectrum of Ca/Al-BC and Mg/Al-BC after phenol adsorption can be seen in Figure 7. Based on these data, it can be known that there is a shift in the wave number in the Ca/Al-BC and Mg/Al-BC material after the phenol adsorption process is carried out which indicates a chemical interaction that occurs in the adsorption process. So, it can be said that the adsorption process does not only occur physically but there is a chemical involvement of adsorption. The adsorption mechanism of phenol on Ca/Al-BC and Mg/Al-BC is represented in Figure 8. According to Ahmad et al. (2023), when the optimum pH ≠ pHpzc, both physical and chemical adsorption occurs. In this study, optimum pH ≠ pHpzc on Ca/Al, Ca/Al-BC, and Mg/Al-BC indicate chemical and physical adsorption occurs. Hydrogen bonds and π-π interactions in aromatic rings in phenols and adsorbents might affect the adsorption process.

4. CONCLUSION

The XRD, FTIR, BET analysis, surface area growth, adsorption ability, and regeneration ability demonstrate the success of the composites Ca/Al-BC and Mg/Al-BC. Composites of Ca/Al-BC and Mg/Al-BC can be employed again in the regeneration process. Mg/Al-BC composites have a higher capacity for adsorption than Ca/Al-BC, according to adsorption studies. The kinetics of PSO and Freundlich isotherms were used in this work to follow the kinetic and isotherm models. Ca-Al/BC and Mg-Al/BC composites can be 5^{th} regenerated with a percent efficiency of 44.2 and 46.67% respectively. Hydrogen bonds and π-π interactions in aromatic rings in phenols and adsorbents might affect the adsorption process.

5. ACKNOWLEDGEMENT

The authors thank to Research Center of Inorganic Materials and Coordination Complexes, Sriwijaya University for support and instrumental analysis.

REFERENCES

Abdel-Gawwad, H. A., M. S. Ahmed, A. H. Mohammed, M. Badawi, A. Bonilla-Petriciolet, E. C. Lima, Y. F. Salama, M. Mobarak, and M. K. Seliem (2023). Utilization of Red Clay Brick Waste in the Green Preparation of an Efficient Porous Nanocomposite for Phenol Adsorption: Characterization, Experiments and Statistical Physics Treatment. *Sustainable Chemistry and Pharmacy*, **32**; 101027

Abdelwahab, O. and N. Amin (2013). Adsorption of Phenol from Aqueous Solutions by *Luffa cylindrica* Fibers: Kinetics, Isotherm and Thermodynamic Studies. *The Egyptian Journal of Aquatic Research*, **39**(4); 215–223

Ahmad, N., F. S. Arsyad, I. Royani, and A. Lesbani (2023). Charcoal Activated As Template Mg/Al Layered Double Hydroxide for Selective Adsorption of Direct Yellow on Anionic Dyes. *Results in Chemistry*, **5**; 100766

Ahmad, N., E. S. Fitri, A. Wijaya, A. Amri, M. Mardiyanto, I. Royani, and A. Lesbani (2022). Catalytic Oxidative Desulfurization of Dibenzothiophene Utilizing Composite Based Zn/Al Layered Double Hydroxide. *Bulletin of Chemical Reaction Engineering & Catalysis*, **17**(4); 733–742

Allwar, A., A. Setyani, U. Sugesti, and K. A. Fauzani (2021). Physical-Chemical Characterization of Nano-Zinc Oxide/Activated Carbon Composite for Phenol Removal from Aqueous Solution. *Bulletin of Chemical Reaction Engineering & Catalysis*, **16**(1); 136–147

Alsamman, L., A. Pich, and M. Möller (2017). Development of Modified Layered Silicates with Superior Adsorption Properties for Uptake of Pollutants from Air and Water. Technical report

Anshar, A. M., P. Taba, and I. Raya (2016). Kinetic and Thermodynamics Studies the Adsorption of Phenol on Activated Carbon from Rice Husk Activated by $ZnCl_2$. *Indonesian Journal of Science and Technology*, **1**(1); 47–60

Asnaoui, H., Y. Dehmani, M. Khalis, and E.-K. Hachem (2022). Adsorption of Phenol from Aqueous Solutions by Na–Bentonite: Kinetic, Equilibrium and Thermodynamic Studies. *International Journal of Environmental Analytical Chemistry*, **102**(13); 3043–3057

Badri, A. F., P. M. S. B. N. Siregar, N. R. Palapa, R. Mohadi, M. Mardiyanto, and A. Lesbani (2021). Mg-Al/Biochar Composite with Stable Structure for Malachite Green Adsorption from Aqueous Solutions. *Bulletin of Chemical Reaction Engineering & Catalysis*, **16**(1); 149–160

Bazrafshan, E., P. Amirian, A. H. Mahvi, and A. Ansari-Moghaddam (2016). Application of Adsorption Process for

© 2023 The Authors.

Phenolic Compounds Removal from Aqueous Environments: A Systematic Review. *Global NEST Journal*, **18**(1); 146–163

Bouteraa, S., F. B. D. Saiah, S. Hamouda, and N. Bettahar (2020). Zn-M-CO_3 Layered Double Hydroxides (M= Fe, Cr, or Al): Synthesis, Characterization, and Removal of Aqueous Indigo Carmine. *Bulletin of Chemical Reaction Engineering & Catalysis*, **15**(1); 43–54

Buhani, M. Puspitarini, Rahmawaty, Suharso, M. Rilyanti, and Sumadirilyanti (2018). Adsorption of phenol and methylene blue in solution by oil palm shell activated carbon prepared by chemical activation. *Oriental Journal of Chemistry*, **34**(4); 2043–2050

Chen, T., T. Da, and Y. Ma (2021). Reasonable Calculation of the Thermodynamic Parameters from Adsorption Equilibrium Constant. *Journal of Molecular Liquids*, **322**; 114980

Chowdhury, A., S. Kumari, A. A. Khan, M. R. Chandra, and S. Hussain (2021). Activated Carbon Loaded with Ni-Co-S Nanoparticle for Superior Adsorption Capacity of Antibiotics and Dye from Wastewater: Kinetics and Isotherms. *Colloids and Surfaces A: Physicochemical and Engineering Aspects*, **611**; 125868

Das, A., A. Jana, D. Das, S. Biswas, H. Sheshadri, M. Rao, and S. De (2023). Surfactant Assisted APTES Functionalization of Graphene Oxide Intercalated Layered Double Hydroxide (LDH) for Uranium Adsorption from Alkaline Leach Liquor. *Journal of Cleaner Production*, **390**; 136058

Dehbi, A., Y. Dehmani, H. Omari, A. Lammini, K. Elazhari, S. Abouarnadasse, and A. Abdallaoui (2020). Comparative Study of Malachite Green and Phenol Adsorption on Synthetic Hematite Iron Oxide Nanoparticles (α-Fe_2O_3). *Surfaces and Interfaces*, **21**; 100637

Dehmani, Y., D. Dridi, T. Lamhasni, S. Abouarnadasse, R. Chtourou, and E. C. Lima (2022). Review of Phenol Adsorption on Transition Metal Oxides and Other Adsorbents. *Journal of Water Process Engineering*, **49**; 102965

Dehmani, Y., O. El Khalki, H. Mezougane, and S. Abouarnadasse (2021). Comparative Study on Adsorption of Cationic Dyes and Phenol by Natural Clays. *Chemical Data Collections*, **33**; 100674

Desmiarti, R., M. Martynis, Y. Trianda, F. Li, A. Viqri, and T. Yamada (2019). Phenol Adsorption in Water by Granular Activated Carbon from Coconut Shell. *Chemical Engineering*, **10**(8); 1488–1497

Haydari, I., K. Aziz, S. Kaya, T. Daştan, N. Ouazzani, L. Mandi, and F. Aziz (2023). Green Synthesis of Reduced Graphene Oxide and Their Use on Column Adsorption of Phenol from Olive Mill Wastewater. *Process Safety and Environmental Protection*, **170**; 1079–1091

Helard, D., S. Indah, C. M. Sari, and H. Mariesta (2018). The Adsorption and Regeneration of Natural Pumice As Low-Cost Adsorbent for Nitrate Removal from Water. *Journal of Geoscience, Engineering, Environment, and Technology*, **3**(2); 86–93

Ho, Z. H. and L. A. Adnan (2021). Phenol Removal from Aqueous Solution by Adsorption Technique Using Coconut Shell Activated Carbon. *Tropical Aquatic and Soil Pollution*, **1**; 98–107

Igwegbe, C. A., A. E. Al-Rawajfeh, H. Al-Itawi, S. Sharadqah, S. Al-Qazaqi, E. Abu Hashish, M. Al-Qatatsheh, and M. Sillanpaa (2019). Utilization of Calcined Gypsum in Water and Wastewater Treatment: Removal of Phenol. *Journal of Ecological Engineering*, **20**(7); 1–10

Juleanti, N., N. R. Palapa, T. Taher, N. Hidayati, B. I. Putri, and A. Lesbani (2021). The Capability of Biochar-Based CaAl and MgAl Composite Materials As Adsorbent for Removal Cr(VI) in Aqueous Solution. *Science and Technology Indonesia*, **6**(3); 196–203

Keshvardoostchokami, M., M. Majidi, A. Zamani, and B. Liu (2021). Adsorption of Phenol on Environmentally Friendly Fe_3O_4/Chitosan/Zeolitic Imidazolate Framework-8 Nanocomposite: Optimization by Experimental Design Methodology. *Journal of Molecular Liquids*, **323**; 115064

Kim, T., K. Yun, N. Kim, B. Cha, J. Han, L. K. Njaramba, S. S. Elanchezhiyan, and C. M. Park (2023). Synthesis of Gelatin Aerogel-Containing Al-Metal Organic Framework for the Removal of Phenolic Contaminants from Aqueous Solutions. *Journal of Water Process Engineering*, **51**; 103441

Kurniawati, D., I. Lestari, Harmiwati, S. Sy, Z. Chaidir, E. Munaf, R. Zein, H. Aziz, and R. Zainul (2015). Biosorption of Pb(II) from Aqueous Solutions Using Column Method by Lengkeng (*Euphoria logan lour*) Seed and Shell. *Journal of Chemical and Pharmaceutical Research*, **7**(12); 872–877

Lammini, A., A. Dehbi, H. Omari, K. ELazhari, S. Mehanned, Y. Bengamra, Y. Dehmani, O. Rachid, A. A. Alrashdi, and O. Gotore (2022). Experimental and Theoretical Evaluation of Synthetized Cobalt Oxide for Phenol Adsorption: Adsorption Isotherms, Kinetics, and Thermodynamic Studies. *Arabian Journal of Chemistry*, **15**(12); 104364

Lee, S. Y., J. W. Choi, K. G. Song, K. Choi, Y. J. Lee, and K. W. Jung (2019). Adsorption and Mechanistic Study for Phosphate Removal by Rice Husk-Derived Biochar Functionalized with Mg/Al-Calcined Layered Double Hydroxides Via Co-Pyrolysis. *Composites Part B: Engineering*, **176**; 107209

Li, L., M. Cheng, L. Qin, E. Almatrafi, X. Yang, L. Yang, C. Tang, S. Liu, H. Yi, and M. Zhang (2022). Enhancing Hydrogen Peroxide Activation of Cu-Co Layered Double Hydroxide by Compositing with Biochar: Performance and Mechanism. *Science of The Total Environment*, **828**; 154188

Liu, X., Y. Tu, S. Liu, K. Liu, L. Zhang, G. Li, and Z. Xu (2021). Adsorption of Ammonia Nitrogen and Phenol onto the Lignite Surface: An Experimental and Molecular Dynamics Simulation Study. *Journal of Hazardous Materials*, **416**; 125966

Mandal, A., P. Mukhopadhyay, and S. K. Das (2019). The Study of Adsorption Efficiency of Rice Husk Ash for Removal of Phenol from Wastewater with Low Initial Phenol Concentration. *SN Applied Sciences*, **1**; 1–13

Mardiah, S. H., D. Arrisujaya, D. Susanty, and N. Yuliani (2022). Preparation, Characterization and Phenol Adsorption of Mangifera kemanga Blume Seed. *Jurnal Sains Natural*, **12**(3); 103–111

Missau, J., D. A. Bertuol, and E. H. Tanabe (2021). Highly Efficient Adsorbent for Removal of Crystal Violet Dye from Aqueous

© 2023 The Authors.

Solution by CaAl/LDH Supported on Biochar. *Applied Clay Science*, **214**; 106297

Mohadi, R., N. R. Palapa, and A. Lesbani (2021). Preparation of Ca/Al-Layered Double Hydroxides/biochar Composite with High Adsorption Capacity and Selectivity toward Cationic Dyes in Aqueous. *Bulletin of Chemical Reaction Engineering & Catalysis*, **16**(2); 244–252

Nakhjiri, M. T., G. B. Marandi, and M. Kurdtabar (2021). Preparation of Magnetic Double Network Nanocomposite Hydrogel for Adsorption of Phenol and P-Nitrophenol from Aqueous Solution. *Journal of Environmental Chemical Engineering*, **9**(2); 105039

Nthunya, L. N., L. Gutierrez, S. Derese, B. B. Mamba, A. R. Verliefde, and S. D. Mhlanga (2019). Adsorption of Phenolic Compounds by Polyacrylonitrile Nanofibre Membranes: A Pretreatment for the Removal of Hydrophobic Bearing Compounds from Water. *Journal of Environmental Chemical Engineering*, **7**(4); 103254

Onder, A., P. Ilgin, H. Ozay, and O. Ozay (2020). Removal of Dye from Aqueous Medium with pH-Sensitive Poly [(2-(acryloyloxy)Ethyl] Trimethylammonium Chloride-Co-1-Vinyl-2-Pyrrolidone] Cationic Hydrogel. *Journal of Environmental Chemical Engineering*, **8**(5); 104436

Palapa, N. R., T. Taher, B. R. Rahayu, R. Mohadi, A. Rachmat, and A. Lesbani (2020). Cual Ldh/Rice Husk Biochar Composite for Enhanced Adsorptive Removal of Cationic Dye from Aqueous Solution. *Bulletin of Chemical Reaction Engineering & Catalysis*, **15**(2); 525–537

Sahmoune, M. N. (2019). Evaluation of Thermodynamic Parameters for Adsorption of Heavy Metals by Green Adsorbents. *Environmental Chemistry Letters*, **17**(2); 697–704

Sahu, J., R. R. Karri, and N. Jayakumar (2021). Improvement in Phenol Adsorption Capacity on Eco-Friendly Biosorbent Derived from Waste Palm-Oil Shells Using Optimized Parametric Modelling of Isotherms and Kinetics by Differential Evolution. *Industrial Crops and Products*, **164**; 113333

Shaji, A. and A. K. Zachariah (2017). Surface Area Analysis of Nanomaterials. In *Thermal and Rheological Measurement Techniques for Nanomaterials Characterization*. Elsevier, pages 197–231

Sun, J., Y. Wang, Y. He, J. Liu, L. Xu, Z. Zeng, Y. Song, J. Qiu, Z. Huang, and L. Cui (2022). Effective Removal of Nanoplastics from Water by Cellulose/MgAl Layered Double Hydroxides Composite Beads. *Carbohydrate Polymers*, **298**; 120059

Tamang, M. and K. K. Paul (2022). Adsorptive Treatment of Phenol from Aqueous Solution Using Chitosan/Calcined Eggshell Adsorbent: Optimization of Preparation Process Using Taguchi Statistical Analysis. *Journal of the Indian Chemical Society*, **99**(1); 100251

Wang, H., D. Zhang, Y. Zhao, and M. Xie (2022). Cationic Surfactant Modified Attapulgite for Removal of Phenol from Wastewater. *Colloids and Surfaces A: Physicochemical and Engineering Aspects*, **641**; 128479

Wang, Y., L. Zhu, H. Jiang, F. Hu, and X. Shen (2016). Application of Longan Shell As Non-Conventional Low-Cost Adsorbent for the Removal of Cationic Dye from Aqueous Solution. *Spectrochimica Acta Part A: Molecular and Biomolecular Spectroscopy*, **159**; 254–261

Wei, L., F. Zietzschmann, L. C. Rietveld, and D. Van Halem (2020). Fluoride Removal by Ca-Al-CO_3 Layered Double Hydroxides at Environmentally-Relevant Concentrations. *Chemosphere*, **243**; 125307

Wei, X., S. Huang, J. Yang, P. Liu, X. Li, Y. Wu, and S. Wu (2023). Adsorption of Phenol from Aqueous Solution on Activated Carbons Prepared from Antibiotic Mycelial Residues and Traditional Biomass. *Fuel Processing Technology*, **242**; 107663

Xie, B., J. Qin, S. Wang, X. Li, H. Sun, and W. Chen (2020). Adsorption of Phenol on Commercial Activated Carbons: Modelling and Interpretation. *International Journal of Environmental Research and Public Health*, **17**(3); 789

Yuliasari, N., A. Wijaya, R. Mohadi, and A. Lesbani (2023). Enhanced Effectiveness on Phenol Removal by MgCr-LDH/Microcrystalline Cellulose Composite and Regeneration Study with Green Desorption Reagent. *Science and Technology Indonesia*, **8**(1); 151–159

Zhou, L., M. Slanỳ, B. Bai, W. Du, C. Qu, J. Zhang, and Y. Tang (2021). Enhanced Removal of Sulfonated Lignite from Oil Wastewater with Multidimensional MgAl-LDH Nanoparticles. *Nanomaterials*, **11**(4); 861

© 2023 The Authors.